Received: 28 February 2020 | Revised: 4 June 2020 | Accepted: 15 June 2020

DOI: 10.1111/ejn.14872

SPECIAL ISSUE ARTICLE

EJN European Journal of Neuroscience FENS WILEY

Neurocan genome-wide psychiatric risk variant affects explicit memory performance and hippocampal function in healthy humans

Anne Assmann[1,2,3] | **Anni Richter**[1] | **Hartmut Schütze**[3,4] | **Joram Soch**[5,6] | **Adriana Barman**[1] | **Gusalija Behnisch**[1] | **Lea Knopf**[1,2] | **Matthias Raschick**[1,2] | **Annika Schult**[1,2] | **Torsten Wüstenberg**[7,8] | **Joachim Behr**[7,9] | **Emrah Düzel**[3,4,10] | **Constanze I. Seidenbecher**[1,10] | **Björn H. Schott**[1,5,10,11]

[1]Leibniz Institute for Neurobiology, Magdeburg, Germany

[2]Department of Neurology, Otto von Guericke University, Magdeburg, Germany

[3]German Center for Neurodegenerative Diseases, Magdeburg, Germany

[4]Institute of Cognitive Neurology and Dementia Research, Otto von Guericke University, Magdeburg, Germany

[5]German Center for Neurodegenerative Diseases, Göttingen, Germany

[6]Bernstein Center for Computational Neuroscience, Humboldt University, Berlin, Germany

[7]Department of Psychiatry and Psychotherapy, Charité University Medicine, Berlin, Germany

[8]Department of Clinical Psychology and Psychotherapy, Institute of Psychology,

Abstract

Alterations of the brain extracellular matrix (ECM) can perturb the structure and function of brain networks like the hippocampus, a key region in human memory that is commonly affected in psychiatric disorders. Here, we investigated the potential effects of a genome-wide psychiatric risk variant in the *NCAN* gene encoding the ECM proteoglycan neurocan (rs1064395) on memory performance, hippocampal function and cortical morphology in young, healthy volunteers. We assessed verbal memory performance in two cohorts (N = 572, 302) and found reduced recall performance in risk allele (A) carriers across both cohorts. In 117 participants, we performed functional magnetic resonance imaging using a novelty-encoding task with visual scenes. Risk allele carriers showed higher false alarm rates during recognition, accompanied by inefficiently increased left hippocampal activation. To assess effects of rs1064395 on brain morphology, we performed voxel-based morphometry in 420 participants from four independent cohorts and found lower grey matter density in the

Abbreviations: ANCOVA, analysis of covariance; ANOVA, analysis of variance; BA, Brodmann area; BD, bipolar disorder; BOLD, blood oxygen level dependent; CNS, central nervous system; CSF, cerebrospinal fluid; DLPFC, dorsolateral prefrontal cortex; DM effect, difference-due-to-memory effect; DNA, deoxyribonucleic acid; ECM, extracellular matrix; EPI, echo-planar image; eQTL, expression quantitative trait loci; fMRI, functional magnetic resonance imaging; FOV, field of view; FWE, family-wise error; FWHM, full width at half maximum; GLM, general linear model; GM, grey matter; GWAS, genome-wide association study; HRF, hemodynamic response function; HWE, Hardy–Weinberg equilibrium; IR-EPI, inversion recovery echo-planer image; LIFG, left inferior frontal gyrus; LTP, long-term potentiation; MANCOVA, multivariate analysis of covariance; MDD, major depressive disorder; MPRAGE, magnetization-prepared rapid acquisition gradient echo; MTL, medial temporal lobe; NCAN, Neurocan gene; PFC, prefrontal cortex; ReML, restricted maximum likelihood; ROI, region of interest; SCZ, schizophrenia; *SEM*, standard error of the mean; SNP, single nucleotide polymorphism; SPGR, spoiled gradient recalled; SPM, Statistical Parametric Mapping; TIV, total intracranial volume; UTR, untranslated region; UV, ultraviolet; VBM, voxel-based morphometry; VLMT, Verbal Learning and Memory Test.

Anne Assmann and Anni Richter contributed equally to this work.

Edited by Alexander Dityatev

The peer review history for this article is available at https://publons.com/publon/10.1111/ejn.14872

University of Heidelberg, Heidelberg, Germany

[9]Department of Psychiatry and Psychotherapy, Medical School Brandenburg, Neuruppin, Germany

[10]Center for Behavioral Brain Sciences (CBBS), Magdeburg, Germany

[11]Department of Psychiatry and Psychotherapy, University Medicine Göttingen, Germany

Correspondence
Björn H. Schott, Leibniz Institute for Neurobiology, Brenneckestr. 6, 39118 Magdeburg, Germany.
Email: bschott@lin-magdeburg.de

Funding information
Leibniz-Gemeinschaft; Deutsche Forschungsgemeinschaft, Grant/Award Number: DFG RI 2964-1, SFB 779 , TP B14 and TP A08; Ministerium für Wissenschaft und Wirtschaft, Land Sachsen-Anhalt

ventrolateral and rostral prefrontal cortex of risk allele carriers. In silico eQTL analysis revealed that rs1064395 SNP is linked not only to increased prefrontal expression of the *NCAN* gene itself, but also of the neighbouring *HAPLN4* gene, suggesting a more complex effect of the SNP on ECM composition. Our results suggest that the *NCAN* rs1064395 A allele is associated with lower hippocampus-dependent memory function, variation of prefrontal cortex structure and ECM composition. Considering the well-documented hippocampal and prefrontal dysfunction in bipolar disorder and schizophrenia, our results may reflect an intermediate phenotype by which *NCAN* rs1064395 contributes to disease risk.

KEYWORDS
episodic memory, extracellular matrix, fMRI, imaging genetics, voxel-based morphometry

1 | INTRODUCTION

In the past decade, genome-wide association studies (GWAS) have yielded multiple common genetic risk factors for the major human psychiatric disorders, particularly schizophrenia (SCZ) and bipolar disorder (BD), but also major depressive disorder (MDD) (Psychiatric GWAS Bipolar Disorder Working Group, 2011; Schizophrenia Psychiatric Genomics GWAS Consortium, 2011; Schulze et al., 2014; Smeland et al., 2019). The A allele of the single-nucleotide polymorphism (SNP) rs1064395 in the *NCAN* gene is one of the best-replicated risk alleles for SCZ (Mühleisen et al., 2012) and BD (Cichon et al., 2011; Wang et al., 2018). A translational study has specifically linked the *NCAN* gene locus to the manic phenotype both in patients carrying the A allele and in *NCAN*-deficient mice (Miró et al., 2012).

NCAN rs1064395 is located on chromosome 19p13 in the 3‘ untranslated region (UTR) of the *NCAN* gene, which encodes the proteoglycan neurocan, expressed specifically in the central nervous system. Neurocan belongs to the family of chondroitin sulphate proteoglycans and is a component of the brain’s extracellular matrix (ECM). Studies in rodents (Meyer-Puttlitz et al., 1995; Zhou et al., 2001) and humans (Schultz et al., 2014) show that neurocan is mainly expressed during brain development, reaching a peak shortly after birth and lower amounts in mature brains. Compatibly with a developmental expression pattern, neurocan has been suggested to be involved in neuronal and glial outgrowth and migration and in axon guidance during post-natal neural development (Berglöf, Plantman, Johansson, & Strömberg, 2008; Rauch, Feng, & Zhou, 2001). Converging evidence from *post-mortem* studies (Chelini, Pantazopoulos, Durning, & Berretta, 2018; Pantazopoulos & Berretta, 2016) as well as neuropsychological and neuroimaging investigations in human patients (Bach, Brown, Kleim, & Tyagarajan, 2019; Piras et al., 2015; Schultz et al., 2014; Wang et al., 2016) points to a role for the ECM in the pathophysiology of SCZ. In animal studies, ECM integrity and composition have been associated with cognitive measures like learning, memory or cognitive flexibility (Banerjee et al., 2017; Gogolla, Galimberti, Deguchi, & Caroni, 2009; Happel et al., 2014), which are often impaired in human psychiatric disorders like SCZ (Preston, Shohamy, Tamminga, & Wagner, 2005; Ragland et al., 2009; Schott et al., 2015; Zierhut et al., 2010).

The hippocampus, which in healthy humans plays a key role in the encoding and retrieval of declarative memory traces (Squire, Stark, & Clark, 2004), shows a volume reduction in patients with SCZ (Bogerts et al., 1993; Vita, de Peri, Silenzi, & Dieci, 2006), which can be already observed during the first episode (Adriano, Caltagirone, & Spalletta, 2012), suggesting that this reflects a developmental phenomenon rather than pathology related to chronic psychiatric illness. In line with this notion, studies in healthy relatives of patients with SCZ, BPD and MDD collectively suggest that hippocampal dysfunction may reflect a heritable risk mechanism for psychiatric disorders (Erk, Meyer-Lindenberg, Linden, et al., 2014; Francis et al., 2013; Skelley,

Goldberg, Egan, Weinberger, & Gold, 2008). Decreased hippocampal volumes (Bearden et al., 2008; Rimol et al., 2010) and deficits in verbal memory (Chepenik et al., 2012) have also been observed in patients with BD, highlighting common neurodevelopmental mechanisms contributing to both SCZ and BD.

Neurocan is strongly expressed in the developing hippocampus (Meyer-Puttlitz et al., 1995; Zhou et al., 2001), and neurocan-deficient mice display a reduced expression of late-phase hippocampal long-term potentiation, a well-established model of hippocampal synaptic plasticity and memory. Considering the converging evidence for structural and functional alterations of the hippocampus and subtle memory impairment in patients with SCZ and BD, it is thus plausible to assume that the psychiatric risk variant *NCAN* rs1064395 A may affect memory performance and hippocampal activity in healthy carriers of the risk allele. In line with this assumption, Raum et al. (2015) reported lower memory performance in A carriers compared to G homozygotes, but did not report genotype-related effects on hippocampal activity. At the level of brain structure, an imaging study in healthy controls and patients with MDD showed lower hippocampal grey matter (GM) density in A carriers, irrespective of diagnosis (Dannlowski et al., 2015). Considering the often poor replication of neuroimaging data, it is important to replicate and expand those results in order to substantiate a potential relationship between *NCAN* genetic variation and altered hippocampal function as an intermediate phenotype for major psychiatric disorders. In the present study, we investigated the effects of *NCAN* rs1064395 on memory performance, using the Verbal Learning and Memory Test (VLMT; Helmstaedter, Lendt, & Lux, 2001) and on memory-related hippocampal activation in a functional magnetic resonance imaging (fMRI) study, using a previously described visual encoding paradigm for novel scenes (Düzel, Schütze, Yonelinas, & Heinze, 2011; Schott et al., 2014). In an additional exploratory analysis, we further aimed to replicate the previously reported genotype-dependent differences in hippocampal and also prefrontal GM density using voxel-based morphometry (VBM).

2 | MATERIALS AND METHODS

We investigated potential effects of *NCAN* rs1064395 on human memory performance using a well-established list-learning test (VLMT; Helmstaedter et al., 2001) in two cohorts. To assess the functional anatomical correlates of a potential effect of *NCAN* rs1064395 on explicit memory performance, an fMRI study was performed, using a previously described paradigm in which novel visual scenes are encoded into episodic memory (Düzel et al., 2011).

2.1 | Subjects

Behavioural data (VLMT) were obtained from two large-scale genetic cohorts conducted at the Department of Psychology, University of Magdeburg (1st cohort; see Richter et al., 2011) and at the Leibniz Institute for Neurobiology in Magdeburg (2nd cohort; see Barman et al., 2014). A health questionnaire previously employed in behavioural genetics research (Krämer et al., 2007; Richter et al., 2011) to exclude history of neurological or psychiatric illness and the use of any centrally acting or illicit drugs accordingly in all participants. To ensure a homogenous educational background, all participants had obtained at least the German university entrance diploma (*Abitur*). Given the verbal nature of the VLMT task, we only considered data from native speakers of German. For a detailed description of the samples see Barman et al. (2014) and Richter et al. (2011). Minor changes in n numbers can be explained by the fact that only complete records were considered for analysis, and, further genetic analyses were no longer possible in 10 subjects from the first cohort.

A total of 120 young (age range 19–34) healthy students from the second cohort were recruited for the fMRI experiment based on availability, exclusion of MRI contraindications and aiming for a balanced gender distribution, but not selected by genotype, to avoid stratification effects. Two participants were excluded from data analysis because of insufficient information regarding past neuropsychiatric illness and one due to abnormalities in the T1-weighted MRI; therefore, the data analysis comprised 117 participants.

Data for the VBM study were pooled from four cohorts of young, healthy participants, yielding a total sample size of $N = 420$. Cohort I included the same participants as the fMRI experiment. Cohort II consisted of participants from previously published imaging genetics studies (Barman et al., 2014; Richter et al., 2011; Schott et al., 2014). The participants from cohorts III and IV belong to an ongoing study and underwent the same MRI protocol as in the DELCODE study (Düzel et al., 2018; Jessen et al., 2018).

Demographic data of all study cohorts are summarized in Table 1. All participants gave written informed consent in accordance with the Declaration of Helsinki and received financial compensation for participation. The work was approved by the Ethics Committee of the University of Magdeburg, Faculty of Medicine. All participants received financial compensation for their participation, which was calculated based on a fixed amount for blood sampling, plus an hourly rate for neuropsychology and neuroimaging studies.

2.2 | Genotyping

Genomic DNA was extracted from EDTA-anticoagulated venous whole blood using the *GeneMole* automated DNA

TABLE 1 Demographic data of both cohorts and fMRI experiment separated by genotype

	GG	AG/AA	Statistics
Behavioural experiment			
1st cohort			
Women/Men	105/99	60/42	$\chi^2_1 = 1.48$; $p = .274$
Mean age ± *SD*	23.1 ± 3.1	22.6 ± 2.7	$F_{1,304} = 1.89$; $p = .17$
2nd cohort			
Women/Men	208/205	88/70	$\chi^2_1 = 1.30$; $p = .26$
Mean age ± *SD*	23.9 ± 2.7	23.6 ± 2.9	$F_{1,569} = 1.25$; $p = .25$
fMRI study			
Cohort I			
Women/Men	40/48	17/12	$\chi^2_1 = 1.51$; $p = .22$
Mean age ± *SD*	24.2 ± 2.5	25.1 ± 2.7	$F_{1,115} = 2.90$; $p = .09$
VBM study			
Cohort I, II, III, IV			
Women/Men	159/153	48/60	$\chi^2_1 = 1.36$; $p = .244$
Mean age ± *SD*	24.1 ± 2.84	24.2 ± 3.14	$t_{418} = -0.49$; $p = .642$
Cohort (I, II, III, IV)	88/165/45/14	29/60/14/5	$\chi^2_3 = 0.28$; $p = .964$
TIV (cm^3) ± *SD*	1,529 ± 141.4	1,502 ± 128.2	$t_{418} = 1.72$; $p = .09$

Note: SD, Standard deviation; TIV, total intracranial volume.

extraction system (Mole Genetics) according to the manufacturer's protocol. Genotyping of *NCAN* rs1064395 was performed using a PCR followed by allele-specific restriction analysis. The DNA fragment containing the rs1064395 polymorphism was amplified using standard PCR methods with the primers *NCAN*-f (5′- CAG TCC TTA AGC AGA CAT TGG TAG TGC C -3′) and *NCAN*-r (5′- GAC TGC TGA AAG TGA GTA ACA GAC ATG GA -3′) (detailed genotyping protocol available upon request). Allele-specific restriction cutting of the G allele was performed with the AciI isoschizomer SsiI (Thermo Fisher Scientific), and the resulting DNA fragments (G: 129 bp + 238 bp; A: 367 bp) were separated on Midori-green-stained agarose gels and visualized under UV light.

2.3 | Behavioural data acquisition and analysis

All subjects of the first and second cohort performed a computer-based version of the VLMT, adapted with minor modifications from the original version of the test (Helmstaedter et al., 2001). Performance of the VLMT was part of a larger-scale neuropsychological testing session (Barman et al., 2014; Richter et al., 2011). Testing was computer-based, and in each learning trial, participants were presented with 15 words. Participants were asked to memorize the words and then write down all words they could remember.

In the first cohort a shortened version of the VLMT was used consisting of three learning trials and an unexpected free-recall test 24 hr after the last presentation of the original word list. In the second cohort the full version was assessed consisting of five learning trials and an interference list at the end. An unexpected free-recall test of the original word list was conducted immediately after the recall of the distractor list and 30 min and 24 hr after the last presentation of the original word list. In all trials, the number of correctly recalled words was the dependent variable of interest. To increase statistical power, we combined both cohorts for statistical analysis, considering only overlapping trials 1 to 3 and the 24-hr delayed recall trial from both cohorts. Data were

analyzed in SPSS with a two-way ANCOVA for repeated measures with memory performance (correctly remembered words in trials 1–3 and in the 24-hr delayed recall task) as within-subject factor, *NCAN* genotype and cohort affiliation (1 vs. 2) as between-subject factors and age and gender as covariates of no interest. *Post hoc* two-sample *t* tests were performed in the case of a significant main effect of genotype in the ANCOVA.

2.4 | FMRI experiment

2.4.1 | Experimental paradigm

117 Participants from the second cohort of the behavioural study underwent a well-established visual memory task in which novel scenes are encoded (Düzel et al., 2011), with minor modifications, as described previously (Schott et al., 2014). Before MRI acquisition one indoor and one outdoor scene (="master pictures") were presented five times each. In the scanner, participants were presented with 88 novel images (44 indoor and 44 outdoor scenes) as well as 22 repetitions of each of the two familiar master pictures. The pictures were presented in a pseudo-random order. Each stimulus was shown for 2.5 s, followed by an average delay of 1,000 ms (jittered with *SD* 500 ms), during which a fixation cross was shown. The order of stimulus presentation was optimized for event-related fMRI time series (Hinrichs et al., 2000). Participants indicated via button press whether an indoor or an outdoor scene was presented. After completing the task, participants underwent further structural MR imaging and, after leaving the scanner, were asked to complete the NEO-FFI personality questionnaire. Approximately 90 min after the start of the fMRI session, a recognition memory task with a five-level confidence rating was performed outside the MR tomograph, during which the 90 images from the fMRI session were presented randomly intermixed with 44 distractors that had not been presented before (22 indoor and outdoor scenes each). Subjects rated their recognition confidence on a scale ranging from 1 to 5 ("1": definitely new; "2": probably new; "3": unsure; "4": probably old; and "5": definitely old). These confidence ratings were used as behavioural measures to form the regressors during first-level fMRI data analysis.

2.4.2 | MRI data acquisition

Structural and functional MRI was acquired using a Verio Syngo 3T MR system (Siemens Medical Systems) with a 32-channel head coil. Prior to the functional MRI session a T1-weigthed sagittal 3D Magnetization Prepared Rapid Acquisition Gradient Echo image (MPRAGE) was acquired (192 slices, 256 × 256 pixel matrix, field of view (FOV) = 256 × 256 mm^2, slice thickness = 1 mm, TE = 4.37 ms, TR = 2,500 ms, flip angle = 7°, voxel size of 1 × 1 × 1 mm^3), followed by the actual fMRI encoding experiment. A total of 206 T2*-weighted echo-planar images (EPIs) were acquired in a single session that lasted approximately 8 min (40 axial slices; in-plane resolution = 104 × 104; FoV = 208 mm × 208 mm; voxel size: 2 × 2 × 3 mm^3; TR = 2,400 ms; TE = 30 ms; flip angle 80°; odd–even interleaved acquisition order). Thereafter, a co-planar T1-weighted inversion recovery echo-planer image (IR-EPI, voxel size = 2 × 2 × 2 mm^3) was acquired for spatial normalization (see below).

2.4.3 | Data processing and analysis

Data analyses were performed using Statistical Parametric Mapping (SPM8; Wellcome Trust Centre for Neuroimaging, Institute of Neurology, London, UK). A detailed description of the analysis has been described previously (Barman et al., 2014; Schott et al., 2014). Briefly, EPIs were corrected for acquisition delay and head motion, normalized to the MNI reference space using the normalization parameters obtained from segmentation of the IR-EPI and smoothed with an isotropic Gaussian kernel of 6 mm at full width half maximum (FWHM). A two-stage mixed effects model was used for statistical analysis, using a previously described protocol to maximize comparability with earlier studies (Barman et al., 2014; Schott et al., 2014). At the first stage, 6 regressors of interest (novel pictures, sorted by later recognition confidence and master pictures) were convolved with the canonical hemodynamic response function provided by SPM, and parameters of the general linear model were estimated using a restricted maximum likelihood fit, with the six movement parameters obtained from motion correction as covariates of no interest. Linear contrast images were computed for the novelty encoding condition (novel stimuli with recognition confidence ratings 4 and 5 compared to the master stimuli) and for the difference-due-to-memory effect (DM effect; stimuli with recognition confidence ratings 4 and 5 compared to stimuli with recognition confidence ratings 1 and 2). The resulting *t* contrasts of parameter estimates were then submitted to a second-level full-factorial random effects model with *NCAN* genotype as fixed factor and age and sex as covariates of no interest. Because of our a priori hypothesis that, in the task at hand, genotype-related effects would most likely be observable in the hippocampus, we performed a region of interest (ROI)-based analysis in the hippocampus bilaterally, using ROIs obtained from the probabilistic cytoarchitectonic atlas (SPM Anatomy Toolbox; Eickhoff et al., 2005). Accordingly, the significance level was set to $p < .05$, family-wise error (FWE)-corrected for the respective ROI with an a priori search threshold of 0.001 (uncorrected) and a minimum cluster size of five voxels. At the second level, we computed an initial *F* contrast of the novelty

effect, comparing *NCAN* genotype groups against each other, and a *t* contrast of the DM effect, based on the direction of the novelty contrast.

2.4.4 | Behavioural data analysis of the fMRI paradigm

The corrected hit rate was computed by subtracting the hit rate (confidence ratings 4 and 5 for pictures displayed in the fMRI scanner) from the rate of false alarms (confidence ratings 4 and 5 to new distractor pictures). A multivariate analysis of covariance (MANCOVA) with hits and false alarms as dependent variables, *NCAN* genotype as between-subject factor and sex and age as covariates was calculated. To control for effects of genotype on the indoor/outdoor scene decision in the encoding phase in the MRI scanner, an additional MANCOVA was conducted with reaction times and error rates (sex and age as covariates). Guided by the results of the experiment by Raum et al. (2015) with worse memory performance in risk allele carriers, we conducted a one-tailed *t* test for hits and the corrected hit rate. As Kolmogorov–Smirnov test showed a significant deviation from normal distribution for false alarms (Kolmogorov–Smirnov-Z = 1.378; $p = .045$), we performed a Mann–Whitney *U* test to test false alarms rate.

2.5 | Brain–behaviour correlations

Guided by the observed association of the *NCAN* A allele with lower memory performance and higher memory-related hippocampal activation, we conducted an exploratory brain–behaviour correlation to further elucidate the relationship between recognition performance and activation of left hippocampus during successful encoding. A power analysis using G*Power (Faul, Erdfelder, Buchner, & Lang, 2009; Faul, Erdfelder, Lang, & Buchner, 2007) suggested that at an expected effect size of $|\rho| = 0.3$ and a power of 0.8, a sample size of 84 subjects would be required. Therefore, we performed the correlational analyses only in the entire sample, but not in the two genotype groups separately. We extracted DM-related fMRI activations (fitted and adjusted response) of the largest activation cluster in the left hippocampus ($[x\ y\ z] = [-30\ -28\ -12]$; the contrast testing subsequently remembered against subsequently forgotten pictures). These values were correlated with individual recognition performance scores (hits, false alarms and corrected hit rates), using Spearman's rank correlations. To verify the reliability of the correlations, we also computed Shepherd's *Pi* correlations, which have been proposed to improve robustness of brain–behaviour correlations. Shepherd's *Pi* correlations are based on Spearman's non-parametric correlation and additionally include a bootstrap-based estimation of the Mahalanobis distance (D_s) and a rejection of data points beyond 6 squared units as outliers, thereby allowing for an unbiased outlier removal (Schwarzkopf, de Haas, & Rees, 2012).

2.6 | Voxel-based morphometry

Genotype-related differences in local cortical morphology were investigated with VBM, employing the Computational Anatomy Toolbox (CAT12; http://www.neuro.uni-jena.de/cat/). To obtain a reasonably large sample size, we pooled data from 420 participants belonging to four cohorts (see above and Table 1, bottom). Participants from cohorts I, III and IV were scanned on Siemens 3T MR systems (cohorts I, III: *Verio*; cohort IV: *Skyra*), and participants from cohort II were scanned on a GE Signa 1.5 MR tomograph (General Electric). In all participants, T1-weighted 3D MR images were acquired at an isotropic resolution of $1 \times 1 \times 1$ mm, using a spoiled gradient-recalled sequence in cohort II, and MPRAGE sequences in the other cohorts (details available upon request).

Data processing and analysis were performed as described previously (Gvozdanovic, Stämpfli, Seifritz, & Rasch, 2020; Weise, Bachmann, Schroeter, & Saur, 2019), with minor modifications. Images were segmented into GM, white matter and cerebrospinal fluid using the segmentation algorithm provided by CAT12. Segmented GM images were normalized to the SPM12 DARTEL template, employing a Jacobian modulation and keeping the spatial resolution at an isotropic voxel size of 1 mm^3. Normalized GM maps were smoothed with a Gaussian kernel of 8 mm at FWHM. Statistical analysis was performed using an ANCOVA model with genotype as fixed factor and age, gender and total intracranial volume (TIV) as covariates. To account for the trend-wise difference in TIV between the two genotype groups (Table 1, bottom) and considering the previously reported influence of TIV on VBM results (Crowley et al., 2018), voxel intensities were proportionally scaled to the mean TIV of all subjects. Genotype-related differences in local GM concentrations were computed as two-sample T contrasts, using a cluster-defining a priori threshold of $p < .001$. We report cluster-level FWE-corrected results at this threshold (Eklund, Nichols, & Knutsson, 2016), and for explorative purposes, additional clusters that came out significant at $p < .001$, uncorrected, with a minimum cluster size of $k = 100$ voxels.

3 | RESULTS

3.1 | Genotype distribution

Among the 306 participants of the first cohort, we identified 10 individuals homozygous for the high-risk allele A of *NCAN* genotype, 92 heterozygotes and 204 G homozygotes.

Genotype distribution did not deviate from Hardy–Weinberg equilibrium (HWE) ($\chi^2 = 0.01$; $p = .92$). In the second cohort, the sample of 571 volunteers included 13 A homozygotes, 145 heterozygotes and 413 G homozygotes. As in the first cohort, there was no significant deviation from HWE ($\chi^2 < 0.01$; $p = .95$). Among the participants of the fMRI experiment, 88 subjects were homozygote for the low-risk allele G and 29 were carriers of the high-risk allele A (27 heterozygotes and two homozygotes). As in the two cohorts of the behavioural experiment, allele frequencies did not deviate from Hardy–Weinberg equilibrium ($\chi^2 = 0.002$; $p = .97$). Across the four cohorts contributing to the VBM study, we identified eight A homozygotes, 100 heterozygotes and 320 G homozygotes. Allele frequencies were at HWE in the pooled cohort ($\chi^2 = 0.003$; $p = .954$) as well as in all subcohorts I to IV (all $\chi^2 < 1.07$; all $p > .301$). Due to the low number of A homozygotes, we compared all A (risk allele) carriers to the G homozygous subjects in all comparisons.

3.2 | Genotype effects on explicit memory performance

3.2.1 | Verbal learning and memory task

A two-way ANCOVA for repeated measures with memory performance (correctly remembered words in trials 1–3 and in the 24-hr delayed recall task) as within-subject factor, *NCAN* genotype and cohort affiliation (1 vs. 2) as between-subject factors and age and gender as covariates of no interest was conducted. As Mauchly's test of sphericity was significant ($\chi^2 = 221.17$; $p < .001$), Greenhouse–Geisser correction was used whenever a factor had more than two levels. ANCOVA revealed a significant main effect of *NCAN* genotype on memory performance ($F_{1,871} = 4.15$; $p = .042$) (Figure 1a, Table 2). There was also a significant main effect of memory ($F_{(2.61;2,275.04)=}19.567$; $p < .001$), reflecting the learning curve from the first to the third trial, and a significant main effect of cohort ($F_{1,871} = 5.29$; $p = .022$), most likely reflecting differences in testing conditions[1] A detailed description of further significant effects of covariates of no interest and significant interactions can be found in Table S1.

3.2.2 | Visual recognition memory (fMRI experiment)

In analogy to the VLMT, high-risk A allele carriers exhibited lower memory performance for visual scenes in the recognition phase of the fMRI experiment compared to participants homozygous for the low-risk G allele (MANCOVA effect of *NCAN* genotype: Wilks' $\Lambda = 0.931$; $p = .018$) driven by the false alarms ($F = 8.31$; $p = .005$). A one-tailed t test showed an effect of *NCAN* genotype on corrected hit rate at trend level ($T = 1.423$; $p = .079$), which was mainly driven by the significant higher rate of false alarms in risk allele carriers ($U = 864.50$; $p = .009$). Hit rates did not differ significantly ($T = 0.13$; $p = .893$). See Figure 1b and Table 2.

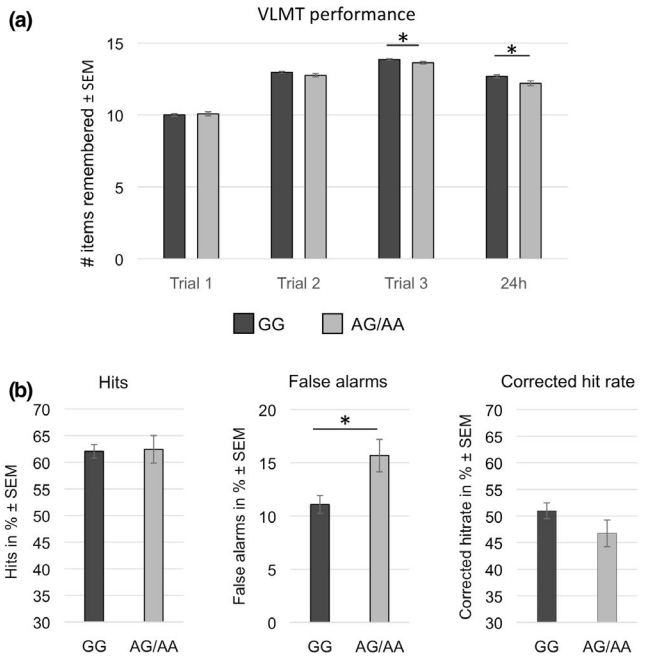

FIGURE 1 Influence of NCAN rs1064395 on recognition: (a) Participants with no risk allele (GG) exhibited a significant higher memory performance in the VLMT. (b) hits, false alarms and corrected hit rates during recognition phase of the fMRI task: risk-allele carriers showed trend-wise lower corrected hit rates ($t = 1.423$; $p = .079$ (one-tailed), mainly driven by significantly higher false alarm rates in risk-allele (A) carriers ($U = 864.50$; $p = .009$)

Importantly, no genotype effects were observed with respect to reaction times or error rates of the indoor/outdoor decision during the encoding phase in the MRI scanner (no MANCOVA effect of *NCAN* genotype: Wilks' $\Lambda = 0.973$; $p = .214$; participants were not instructed to respond as fast as possible).

3.3 | Genotype effects on memory-related hippocampal activity

All fMRI results are based on a comparison of the first-level novelty and DM effect contrasts between the genotype groups. We first report neural correlates of novelty and successful encoding for the sake of comparability with previous studies, followed by differences between the genotype groups.

[1]Cohort 1 was investigated in a classroom-like setting (approx. 20 subjects per session), while the testing in Cohort 2 was performed in a smaller testing room with a maximum of five participants per session.

TABLE 2 Behavioural data

	GG	AA/AG	Statistics	Cohen's *d*
VLMT				
Trial 1	10.01 ± 2.34	10.08 ± 2.24	$T = -0.374$; $p = .708$	0.03056
Trial 2	12.97 ± 1.87	12.76 ± 1.90	$T = 1.546$; $p = .122$	0.11140
Trial 3	13.86 ± 1.44	13.63 ± 1.54	$T = 2.084$; $p = .037$	0.15428
Trial 24h	12.69 ± 2.57	12.20 ± 2.83	$T = 2.371$; $p = .018$	0.18127
fMRI task				
Corrected hit rate	50.98 ± 14.01	46.75 ± 13.50	$T = 1.423$; $p = .157$	0.30747
Hits	62.06 ± 12.10	62.42 ± 13.98	$T = -0.134$; $p = .893$	0.02754
False alarms	11.08 ± 7.87	15.67 ± 8.20	$U = 864.50$; $p = .009$	0.57113

Note: VLMT: Number of correct remembered words ± standard deviation (*SD*). FMRI task: corrected hit rate, hits and false alarms in percent ± *SD*. *p* values of the *T* tests are indicated two-tailed.

3.3.1 | General neural correlates of novelty encoding processing and DM effect

As expected, the analysis of the novelty contrast (BOLD response to novel stimuli with subsequent recognition confidence ratings 4 and 5 compared to the "master" scenes) revealed significant activations in the left hippocampus ([*x y z*] = [−20 −16 −20]; $T_{111} = 9.52$; $p < .001$, whole-brain FWE-corrected, cluster size = 60 voxels) and the right parahippocampal gyrus ([*x y z*] = [26 −42 −14]; $T_{111} = 24.20$; $p < .001$; whole-brain FWE-corrected) independently of *NCAN* genotype. Further significant activations were registered in the dorsolateral and medial prefrontal cortex (BA 11 + 46) as well as in the cingulate gyrus. For further information see Table S2.

When analyzing the DM (difference-due-to-memory) effect (BOLD response to novel stimuli with subsequent recognition confidence ratings 4 and 5 compared to those with recognition confidence 1 and 2) significant brain activations were observed in the left parahippocampal gyrus ([*x y z*] = [−26 −44 −14]; $T_{111} = 6.55$; $p < .001$; whole-brain FWE-corrected, cluster size = 44 voxels) and the right parahippocampal gyrus ([*x y z*] = [24 −40 −14]; $T_{111} = 6.57$; whole-brain FW-corrected, cluster size = 41 voxels). For further information see Table S3.

3.3.2 | Genotype effects on novelty encoding and subsequent memory effect

An ANCOVA with *NCAN* genotype as fixed factor and sex and age as covariates of no interest revealed a significant main effect of genotype on left hippocampal activation in the novelty contrast ([*x y z*] = [−30 −28 −10]; $F = 16.76$; $p = .022$) with high-risk A allele carriers showing a significantly higher hippocampal activation (Figure 2a). The same effect could be observed examining the DM effect (comparison of later remembered words with confidence rating 4 and 5 compared to later forgotten words with confidence rating 1 and 2). In this condition, high-risk allele carriers showed likewise a significantly higher hippocampal activation ([*x*, *y*, *z*] = [−30, −28, −12]; $T = 3.80$; $p = .029$) (Figure 2b).

3.3.3 | Brain –behaviour correlations

When correlating the fMRI response of the hippocampal activation during successful memory formation (DM effect) with the memory performance (corrected hit rates) in the recognition phase, we found higher left hippocampal activation during encoding to exhibit a significant negative correlation associated with memory performance (Spearman's $\rho = -0.285$; $p = .0018$). This correlation remained significantly negative when performing an unbiased outlier exclusion based on the Mahalanobis distance (Shepherd's *Pi* correlation; Schwarzkopf et al., 2012; see Figure 2c). When directly correlating the hippocampal DM responses with hits, the correlation was negative, but did not reach significance (Spearman's $\rho = -0.131$; $p = .159$). False alarms showed a marginally significant positive correlation with the hippocampal response (Spearman's $\rho = 0.182$; $p = .0493$), but this was no longer significant after outlier exclusion ($p = .261$).

3.4 | Genotype effects on human cortical anatomy

Using VBM as implemented the CAT12 toolbox, we aimed to assess potential differences in local GM distribution between *NCAN* genotype G homozygotes and A carriers. While we detected no differences in GM density in the hippocampus

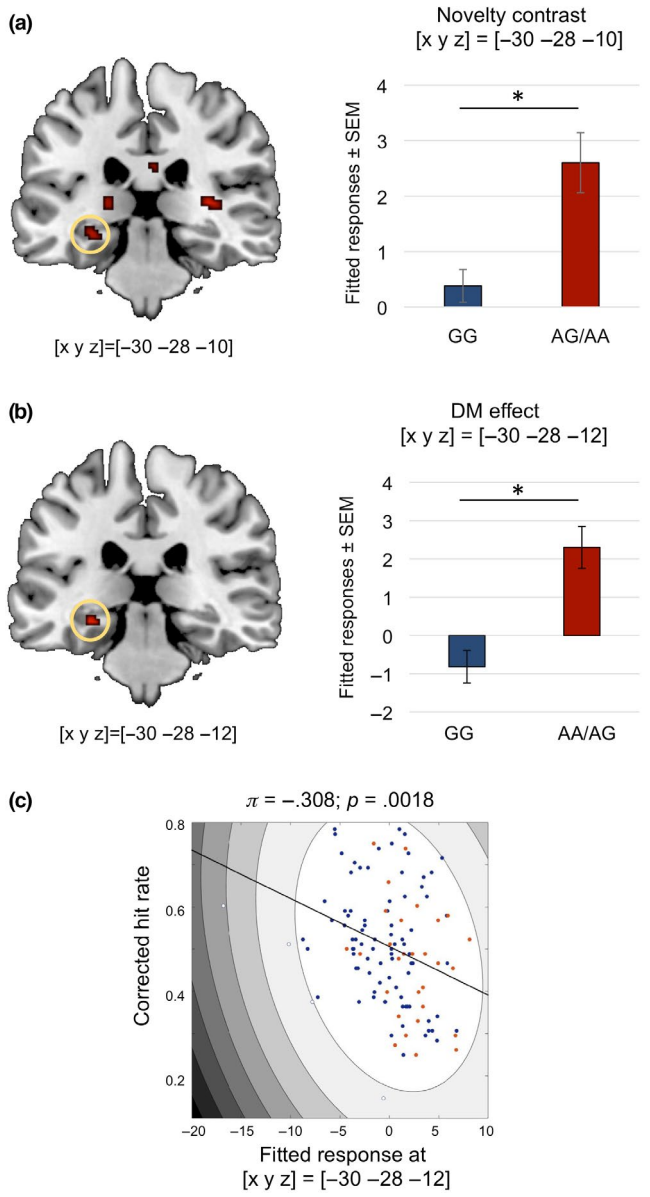

FIGURE 2 Modulation of memory-related hippocampal activity by NCAN genotype: (a) allele carriers showed a significantly higher hippocampal activation during novelty encoding ($F = 16.76$; $p = .022$ FWE-corrected for hippocampal ROI volume) and when comparing in the recognition phase correctly remembered items versus later forgotten pictures (DM effect; T = 3.80; $p = .029$ FWE-corrected for ROI volume). Coordinates are in MNI space; bar plots depict SPM contrasts for the remembered versus forgotten scenes, separated by genotypes. Error bars depict standard error of the mean. (c) Increased hippocampal activation during successful encoding was negatively correlated with recognition performance (corrected hit rate). The plot depicts an outlier-robust Shepherd's *pi* correlation (Schwarzkopf et al., 2012). Data points of G homozygotes are shown in blue, and data points of A carriers are shown in red.

or adjacent medial temporal lobe (MTL) structures, we found that A carriers showed lower GM density in three regions within the prefrontal cortex (PFC; Figure 3). The largest and most robustly significant cluster ($p < .05$, whole-brain FWE-corrected at cluster level with an a priori significance level of $p < .001$) encompassed portions of the left ventrolateral PFC (VLPFC), mostly the left inferior frontal gyrus (LIFG), pars triangularis (BA 44, 45; [*x y z*] = [−49 8 2]), and extended into the left frontal operculum (BA 44) and the most anterior portions of the left insula. In a further exploratory analysis ($p < .001$, uncorrected, with a minimum cluster size of 100 voxels), we observed two smaller clusters within the PFC (Table 3). One was located in the right frontopolar cortex (BA 10; [*x y z*] = [12 74 16]), and the other extended from the left VLPFC into the precentral gyrus (BA 44; [*x y z*] = [−72 2 24]).

3.5 | Expression quantitative trait loci (eQTLs) linked with *NCAN* rs1064395

To link our genotype-dependent behavioural and brain structural and functional data to the potential molecular consequences of the SNP, we performed an eQTL analysis for gene expression changes. In 2016, Wang et al. (2016) published significantly increased neurocan expression in the frontal cortex of A allele carriers, based on eQTL data from the BrainEAC database. However, due to the small sample size (95 GG, 37 GA, 2 AA), the statistical significance was rather poor ($p = .0022$). Here, we conducted eQTL analyses in the eQTL BrainSeq database (Schubert et al., 2015; http://eqtl.brainseq.org/) and found a moderate association of the A allele with NCAN expression levels in the dorsolateral prefrontal cortex (DLPFC) ($p = 3.2559e\text{-}4$, FDR = 3.0763e-2).

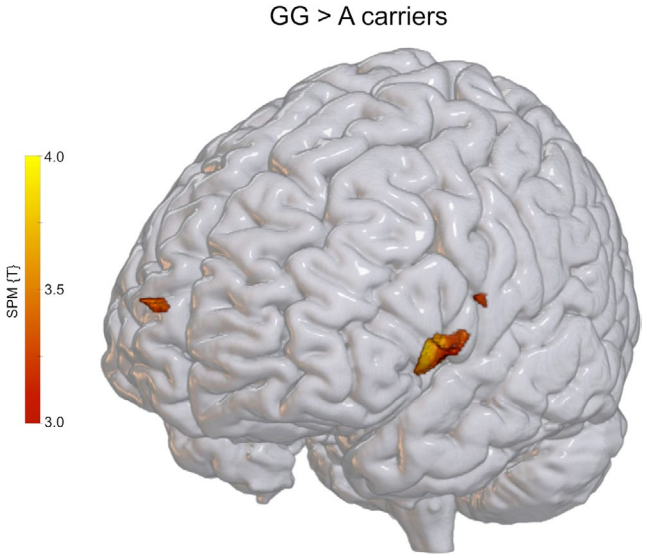

FIGURE 3 NCAN rs1064395 and prefrontal grey matter density. A allele carriers showed significantly reduced grey matter density in the left ventrolateral PFC ($p < .05$, family-wise error-corrected at cluster level) and, to a lesser degree, also in the right rostral PFC (minimum cluster size = 100 voxels). Cluster-defining threshold $p < .001$, uncorrected

TABLE 3 Genotype-related differences in grey matter density

Structure	BA	Cluster size	[x y z]	SPM{T}
GG > A carriers				
Left inferior frontal gyrus/ frontal operculum	44,45	1,340*	−50 12 2	3.97
Left anterior insula	45		−46 2 0	3.82
Left rolandic operculum	44		−54 2 8	3.39
Right medial frontal gyrus	9, 10	353	12 74 16	4.21
Right superior frontal gyrus	9, 10		16 68 18	3.41
Left postcentral gyrus	44	179	−70 2 24	3.86
	44		−58 0 18	3.36
A carriers > GG				
Left cerebellum/vermis		287	−4 −44 −34	3.83
Left cerebellum		134	−6 −62 −63	3.51
		122	−6 −58 −50	3.29

Note: Clusters of significant grey matter density are reported at $p < .001$, uncorrected, with a minimum cluster size of $k = 100$ voxels.

BA, Brodmann area.

[a]All clusters are reported at $p < .001$, uncorrected, with a minimum cluster size of k = 100 voxels. $p < .05$, FWE-corrected at cluster level.

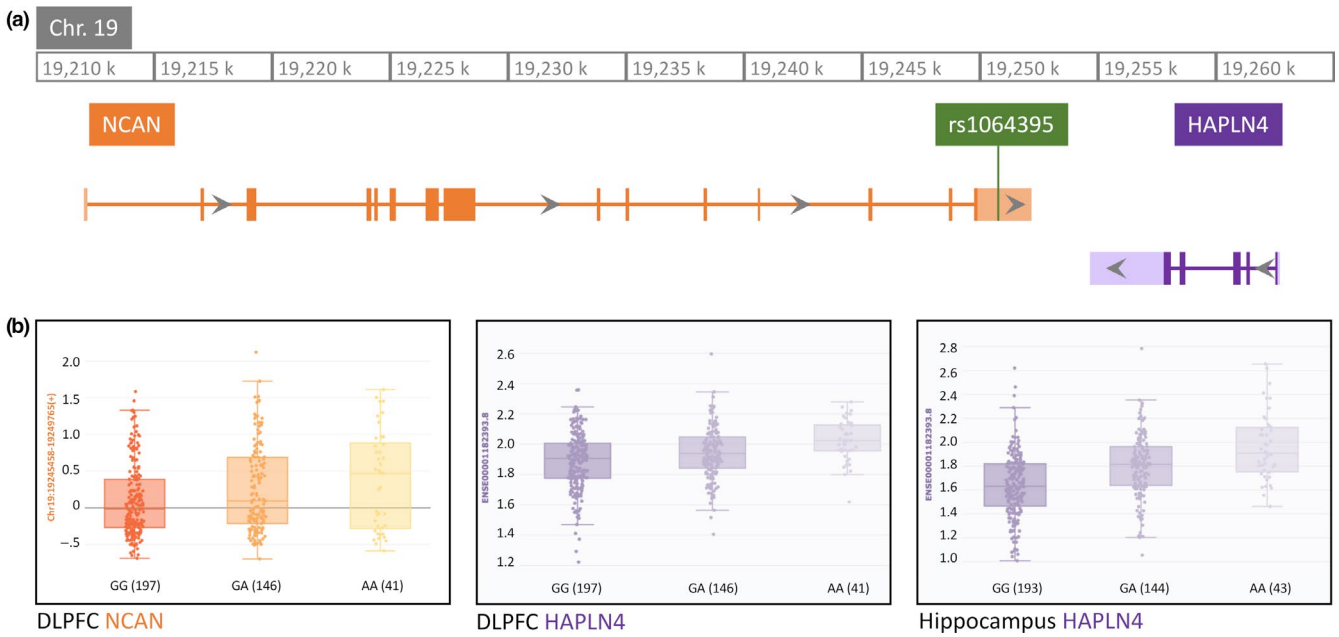

FIGURE 4 Gene locus of rs1064395 and potential effects on ECM gene expression. (a) Alignment of the SNP rs1064395 to the 3' untranslated region of the human NCAN gene located on chromosome 19. The neighbouring inversely oriented HAPLN4 gene is also depicted. (b) eQTL analysis of the SNP rs1064395 in the eQTL Brainseq database (http://eqtl.brainseq.org/) has revealed significant effects on the expression of NCAN in the DLPFC, but also on HAPLN4 expression in DLPFC and hippocampus of risk allele carriers

Interestingly, the expression of the neighbouring *HAPLN4* gene encoding the ECM link protein Hapln4/Bral2 (Figure 4a) correlated with the *NCAN* SNP rs1064395 with much higher statistical significance both in the DLPFC (p = 3.1169e-7, FDR = 6.5569e-5; replication in first phase BrainSeq: p = 1.534e-12, FDR = 3.068e-10) and in the hippocampus (p = 4.1180e-17, FDR = 5.1398e-14; same allelic direction in the GTEx project) (Figure 4b).

4 | DISCUSSION

Our study provides evidence for an effect of *NCAN* rs1064395 on memory performance and hippocampal function in young, healthy adults. We could replicate previous results (Raum et al., 2015) that *NCAN* rs1064395 is associated with lower memory performance. Specifically, individuals carrying the *NCAN* psychiatric risk allele A showed a significantly lower memory performance during delayed verbal recall and a higher false alarm rate during recognition of scene stimuli. In our fMRI study, we found a significant association of *NCAN* rs1064395 with hippocampal activation during encoding, with A carriers showing inefficiently increased hippocampal activation in both the novelty contrast (novel vs. highly familiar scenes) and the DM contrast (later recognized pictures vs. forgotten scenes). Finally, using VBM, we found that A carriers showed lower GM density in the ventrolateral and rostral prefrontal cortex.

4.1 | Effect of *NCAN* genotype on hippocampus-dependent memory

Our observation of lower performance in the delayed recall phase of the VLMT replicates a previous study by Raum et al. (2015), who also found an association of the A allele with poorer immediate and free recall performance in the same memory test. Furthermore, we also observed higher false alarm rates and, as a result, trend-wise lower corrected hit rates in rs1064395 A carriers during the recognition phase of the scene encoding task performed in the fMRI study. Together with the findings by Raum et al. and a study reporting a deleterious effect of the A allele on memory performance in patients with SCZ (Wang et al., 2016), our results provide converging evidence for a role of the *NCAN* genomic locus in human hippocampus-dependent memory. The effect sizes observed in our present study (Table 2) were lower than those reported by Raum et al. (2015), which were in a range of $0.51 < \text{Cohen's } d < 0.62$.[2] This is of note when considering that the sample size contributing to the VLMT data was substantially larger in our study ($N = 877$ vs. 110). One likely reason for this is a difference in sample homogeneity. While Raum and colleagues included individuals of a rather broad age range (18–56) and from different educational backgrounds (mean years of education ~11.8 years), our sample was very homogeneous, consisting solely of students or university graduates with at least a high school diploma (German *Abitur* or similar) and age of 18–35 years. In such a homogenous sample, effect sizes of genetically mediated differences should be expected to be low. Moreover, a common phenomenon in genetic association studies, but not limited to these, is that effect sizes tend to be relatively large in the initial reports and turn out to be smaller in replications and meta-analyses (Ioannidis, 2008). This phenomenon is particularly common in small, and thus likely underpowered, samples (Button et al., 2013), Therefore, while the replicability of the association between the *NCAN* psychiatric risk variant and explicit memory performance is so far encouraging with three studies reporting converging results (Raum et al., 2015; Wang et al., 2016, and the present study), further replications and perspectively meta-analyses will be required to estimate the true strength of the observed association.

To further elucidate how the *NCAN* psychiatric risk variant might exert its influence on memory processing, we investigated its effects on hippocampal function during the processing of novel scene stimuli and their encoding into episodic memory using fMRI. The task employed has previously been evaluated extensively and provides a useful measure to assess altered brain activity patterns during encoding in relation to aging (Düzel et al., 2011) and genetics (Barman et al., 2014; Schott et al., 2014). Analyses of novelty processing and successful encoding (DM effect) yielded significant activations in the bilateral hippocampus and parahippocampal gyrus, in line with previous findings (Düzel et al., 2011). Notably, A carriers exhibited increased rather than decreased hippocampal activation during novelty processing and successful encoding compared to G homozygotes. In both contrasts, the novelty contrast and the DM contrast, only successfully encoded (i.e. later remembered) items were compared to either the highly familiar master images (novelty contrast) or the subsequently forgotten novel images (DM contrast). The relative hyperactivation of the left hippocampus in A carriers during successful encoding (DM) further showed a significant negative correlation with memory performance. This may at first seem counterintuitive, but it should be noted that the DM contrast already reflects a differential rather than an absolute hippocampal activation, suggesting that A carriers, who exhibit lower memory performance, may show additional recruitment of the hippocampus as compensatory mechanism to achieve encoding success.

A number of studies have assessed the modulation of hippocampal activity during encoding and retrieval by genetically mediated individual differences. While gene variants of, for example, CACNA1C, PCLO or RASGRF1 have been associated with reduced activation of the hippocampus in carriers of the allele associated with poorer memory performance (Barman et al., 2014; Schott et al., 2014) or increased risk of psychiatric illness (Erk, Meyer-Lindenberg, Linden, et al., 2014; Erk et al., 2010), other studies, for example on BDNF and COMT (Fera et al., 2013; Krach et al., 2010; Wegman, Tyborowska, Hoogman, Arias Vásquez, & Janzen, 2017),

[2]Raum et al. did not report effect sizes in their article from 2015, and Cohen's *d* values were calculated by the authors of the present study based on the descriptive statistics reported by Raum et al. (i.e., means, standard deviations, and sample sizes).

have revealed increased hippocampal activation in carriers of the presumed risk alleles. There is, thus far, little agreement with respect to the memory-related contrasts that are employed in imaging genetics studies of human memory. Some studies have compared high to low memory conditions (e.g. Bertolino et al., 2006; Erk, Meyer-Lindenberg, Linden, et al., 2014), while others have employed subsequent memory contrasts (Barman et al., 2014; Schott et al., 2006). Therefore, in addition to the specific genes investigated, one potential explanation for the discrepancy regarding increased versus decreased hippocampal activation in carriers of the presumed risk allele observed in imaging genetics studies of hippocampus-dependent memory may also be related to the specific contrasts tested.

4.2 | Hippocampal dysfunction in psychosis risk and a potential role for the ECM

Previous neuroimaging studies have shown altered neural activation patterns related to episodic memory and novelty processing in patients with SCZ (Oertel-Knöchel et al., 2014; Preston et al., 2005; Ragland et al., 2009; Schott et al., 2015; Zierhut et al., 2010) and also BD. Those results are mirrored by similar findings in individuals at high psychosis risk (Lieberman et al., 2018) and in unaffected relatives of patients with SCZ (Christodoulou, Messinis, Papathanasopoulos, & Frangou, 2012; Saleem, Kumar, & Venkatasubramanian, 2018), demonstrating that they may reflect a risk state rather than an effect of the disease itself. Furthermore, unaffected relatives and carriers of a genetic risk variant in the CACNA1C gene exhibit qualitatively similar alterations of memory-related frontolimbic network activity (Erk, Meyer-Lindenberg, Schmierer, et al., 2014), supporting the notion that genetically driven risk mechanisms for psychiatric disorders may be even observable in healthy allele carriers of single risk variant.

The precise role of the hippocampus and MTL memory system in the pathogenesis of psychotic disorders is a matter of ongoing debate. While hippocampal volumes are typically reduced in patients with SCZ compared to healthy controls even at a very early stage of the disorder (Bartsch, Schott, & Behr, 2019; Bogerts et al., 1990), hippocampal neural activity has been suggested to be tonically increased, and this increase is inversely associated with cognitive performance (Friston, Liddle, Frith, Hirsch, & Frackowiak, 1992; Schobel et al., 2009; Suazo, Díez, Tamayo, Montes, & Molina, 2013; Talati et al., 2014; Tregellas et al., 2014). While patients with SCZ usually show only moderate memory deficits, several authors have emphasized the role of the hippocampus in the manifestation of the core clinical features of psychosis like delusions and hallucinations, which are collectively referred to as positive symptoms (for two recent reviews, see Bartsch et al., 2019; Lieberman et al., 2018). One mechanism underlying this phenomenon may be that hippocampal hyperfunction promotes mesolimbic dopamine release (Bartsch et al., 2015; Lisman & Grace, 2005; Lisman et al., 2008; Lodge & Grace, 2007). Notably in this context, ECM proteoglycans modulate the outgrowth of dopaminergic midbrain neurons during development (Berglöf et al., 2008), and D1 type dopamine receptor activation can promote proteolysis of ECM components (Mitlöhner et al., 2020). The interaction between the ECM and the dopaminergic system may thus provide an interesting candidate mechanism for the molecular pathophysiology of SCZ. While those concepts are primarily derived from animal models, it should be noted that both disproportional hippocampal engagement during episodic encoding (Zierhut et al., 2010) and altered hippocampal–frontolimbic functional connectivity during novelty processing (Schott et al., 2015) have been associated with severity of positive symptoms. A limitation of the present study is that we did not assess subclinical traits of psychosis proneness (e.g. schizotypy). Future studies should be investigated to what extent atypical hippocampal and frontolimbic response patterns in individuals at genetic risk of psychosis might be related to subclinical psychosis-related traits.

4.3 | Neurocan genetic variant and prefrontal cortex structure

Despite the observed relationship between *NCAN* rs1064395 and human memory performance and the dysfunctional hippocampal activation found in A carriers, we did not observe an effect of the polymorphism on hippocampal morphology, as previously reported (Dannlowski et al., 2015). We could, however, replicate the finding from the same study that rs1064395 was associated with reduced circumscribed prefrontal GM density in healthy carriers of the A allele. Similar to our findings, Dannlowski and colleagues also observed lower GM concentrations in the LIFG and in the right anterior PFC of A allele carriers. More recently, *NCAN* rs1064395 has also been suggested to affect white matter volume in several brain regions in young adults and infants, including the left inferior prefrontal cortex (Einarsdottir et al., 2017). An earlier study by Schultz et al. (2014) had reported reduced cortical folding in the left dorsolateral PFC in patients with SCZ, but not in healthy controls. It should be noted, though, that the sample size in that study ($N = 65$) may have been too small to detect subtle genetically mediated differences in cortical morphology in a psychiatrically healthy population. Reduced ventrolateral and rostral PFC GM has been reported in patients with SCZ compared to both healthy controls and patients with BD (Nenadic et al., 2015) as well in BD patients with compared to those without history of psychotic symptoms (Ekman et al., 2017). In a meta-analysis of VBM

studies in patients with SCZ and their unaffected relatives (Palaniyappan, Balain, & Liddle, 2012), the medial PFC (in vicinity of the frontopolar cluster identified here) was among the brain structures showing reduced GM density as a function of disease diathesis (relatives < controls), whereas the LIFG was one of the regions with reduced GM density related to disease expression (patients < relatives). While all participants of the present study were young, healthy individuals, the observation that *NCAN* A allele carriers showed reduced GM density in both the LIFG and the right (medial) frontopolar cortex provides further support for subtle structural alterations in these parts of the PFC in the risk development for SCZ and possibly other major psychiatric disorders like BD. Notably in this context, reduced frontopolar and ventrolateral prefrontal activation during episodic encoding has been found in a meta-analysis of fMRI studies in patients with SCZ (Ragland et al., 2009), providing further evidence for a role of these parts of the PFC in the pathophysiology of psychotic disorders.

An additional explanation for the observed prefrontal GM reductions in A carriers may be related to the neuroinflammation hypothesis of SCZ (Buckley, 2019), which has recently gained considerable attention. In a *post-mortem* study of multiple sclerosis (MS), a paradigmatic neuroinflammatory disorder, Fransen et al. (2020) found that carriers of the A allele of *NCAN* rs1064395 exhibited a higher incidence of cortical GM lesions compared to G homozygotes. While neuroinflammatory activity in SCZ does by no means reach the degree of inflammation regularly found in MS, future research should nevertheless explore the possibility of neuroimmunological dysregulation as a potential factor contributing to the observed effects of the *NCAN* polymorphism.

4.4 | Potential underlying cellular mechanisms

The human *NCAN* gene is located on chromosome 19p12-13.1 in close neighbourhood to the inversely oriented HAPLN4 gene encoding the ECM link protein Hapln4/Bral2 (Bekku et al., 2003; Spicer, Joo, & Bowling, 2003). The product of this gene is another important constituent of brain ECM. It binds to hyaluronic acid and largely colocalizes with brevican, one of the major brain proteoglycans (Bekku et al., 2003). Hapln4 has been shown to be strongly expressed in normal human cortex, but its expression is decreased in high-grade glioma samples (Sim, Hu, & Viapiano, 2009). Studies report an impact of Hapln4/Bral2 deficiency on extracellular space architecture and diffusion properties in several brain areas in HAPLN4 knockout mice (Cicanic et al., 2018; Sucha et al., 2020). Thus, the eQTL results presented here point to a rather complex scenario of potentially subtle ECM modifications comprising not only (if at all) the *NCAN* gene product itself but also a hyaluronan link protein and potentially also brevican as Hapln4 partner molecule in brain ECM perineuronal nets.

5 | LIMITATIONS

One limitation of the current study is related to the analysis of the fMRI data. To maximize comparability with previous studies using the same experimental paradigm (Barman et al., 2014; Schott et al., 2014), we computed differential contrasts of interest (novelty, DM) at the first level. Therefore, no main effects of genotype independent of these contrasts could be computed. It should be noted, though, that the use of differential contrasts, such as high versus low memory conditions (Bertolino et al., 2006; Erk, Meyer-Lindenberg, Linden, et al., 2014; Kauppi, Nilsson, Adolfsson, Eriksson, & Nyberg, 2011) or subsequently remembered versus subsequently forgotten items (Barman et al., 2014; Schott et al., 2006), in second-level analyses is currently the most common approach in imaging genetics studies of human memory. A more recently used alternative approach is the use of encoding success as a parametric modulator (Richter et al., 2017), which should be further explored in the future.

Another limitation concerns the brain–behaviour correlation, which was only computed across the entire study sample (Figure 2c). While the observed correlation supported our assumption that increased hippocampal activation in relation to the *NCAN* polymorphism was to some degree inefficient, separate correlations for each genotype group might have been more informative. However, power analysis suggested that the sample sizes would be likely too small, particularly in the group of A carriers. Yarkoni noted that the power to detect a correlation of $r = .2$ with a significance level of $p < .05$ would be as low as about 0.2 (see Yarkoni, 2009, Figure 1). Button et al. (2013) have further pointed out that low power increases the risk of reporting not only false-negative but also false-positive results, as it decreases the positive predictive value. Therefore, the brain–behaviour correlations were not performed separately for the genotype groups.

6 | CONCLUSIONS

Our results provide evidence for a role of the genome-wide psychiatric risk variant *NCAN* rs1064395 in human hippocampus-dependent memory. Carriers of the high-risk A allele exhibit lower memory performance, but atypically increased hippocampal activity during episodic encoding. Furthermore, the A allele could be linked to decreased PFC volume and higher expression of NCAN and of the neighbouring ECM gene *HAPLN4* in the PFC, pointing to a complex scenario of developmentally manifested ECM and brain

structure–function alterations. The present study thereby provides further evidence for the pivotal role of ECM-encoding gene loci in the establishment of intermediate phenotypes of neuropsychiatric disorders.

ACKNOWLEDGEMENTS

The authors would like to thank Ina Schanze for help with obtaining blood samples. We further thank Anna Deibele, Marieke Klein, Catherine Libeau, Jacqueline Mertha and Carola Nath for assistance with data analysis and Kerstin Möhring, Katja Neumann, Ilona Wiedenhöft and Claus Tempelmann for assistance with MRI acquisition. This study was supported by the Deutsche Forschungsgemeinschaft (SFB 779, TP A08, B14) and by the State of Saxony-Anhalt and the European Union (Research Alliance "Autonomy in Old Age"). A.A. and A.B. were members of the Leibniz Graduate School "Synaptogenetics" funded by the Leibniz Association. A.R. was supported by a DFG research stipend (DFG RI 2964-1). L.K. and A.A. were supported by a fellowship from the Otto von Guericke University Medical Faculty.

CONFLICT OF INTEREST

The authors declare that the research was conducted in the absence of any commercial or financial relationships that could be construed as a potential conflict of interest.

DATA AVAILABILITY STATEMENT

Tables with anonymized VLMT results as well as behavioural data of the fMRI experiment and peak hippocampal activations are provided in Excel format as supplementary online material. Anonymized image data from the fMRI and VBM experiments are available from the authors upon reasonable request.

ORCID

Joram Soch https://orcid.org/0000-0002-8879-5666
Torsten Wüstenberg https://orcid.org/0000-0001-8408-2864
Björn H. Schott https://orcid.org/0000-0002-8237-4481

REFERENCES

Adriano, F., Caltagirone, C., & Spalletta, G. (2012). Hippocampal volume reduction in first-episode and chronic schizophrenia: A review and meta-analysis. *The Neuroscientist: A Review Journal Bringing Neurobiology, Neurology and Psychiatry*, *18*, 180–200. https://doi.org/10.1177/1073858410395147

Bach, D., Brown, S. A., Kleim, B., & Tyagarajan, S. (2019). Extracellular matrix: A new player in memory maintenance and psychiatric disorders. *Swiss Medical Weekly*, *149*, w20060. https://doi.org/10.4414/smw.2019.20060

Banerjee, S. B., Gutzeit, V. A., Baman, J., Aoued, H. S., Doshi, N. K., Liu, R. C., & Ressler, K. J. (2017). Perineuronal nets in the adult sensory cortex are necessary for fear learning. *Neuron*, *95*, 169–179. e3. https://doi.org/10.1016/j.neuron.2017.06.007

Barman, A., Assmann, A., Richter, S., Soch, J., Schütze, H., Wüstenberg, T., … Schott, B. H. (2014). Genetic variation of the RASGRF1 regulatory region affects human hippocampus-dependent memory. *Frontiers in Human Neuroscience*, *8*, 260. https://doi.org/10.3389/fnhum.2014.00260

Bartsch, J. C., Fidzinski, P., Huck, J. H., Hortnagl, H., Kovacs, R., Liotta, A., … Behr, J. (2015). Enhanced dopamine-dependent hippocampal plasticity after single MK-801 application. *Neuropsychopharmacology: Official Publication of the American College of Neuropsychopharmacology*, *40*, 987–995. https://doi.org/10.1038/npp.2014.276

Bartsch, J. C., Schott B. H., Behr J. (2019). Hippocampal Dysfunction in Schizophrenia and Aberrant Hippocampal Synaptic Plasticity in Rodent Model Psychosis: a Selective Review. *Pharmacopsychiatry*. https://doi.org/10.1055/a-0960-9846

Bearden, C. E., Thompson, P. M., Dutton, R. A., Frey, B. N., Peluso, M. A. M., Nicoletti, M., … Soares, J. C. (2008). Three-dimensional mapping of hippocampal anatomy in unmedicated and lithium-treated patients with bipolar disorder. *Neuropsychopharmacology: Official Publication of the American College of Neuropsychopharmacology*, *33*, 1229–1238. https://doi.org/10.1038/sj.npp.1301507

Bekku, Y., Su, W.-D., Hirakawa, S., Fässler, R., Ohtsuka, A., Kang, J. S., … Oohashi, T. (2003). Molecular cloning of Bral2, a novel brain-specific link protein, and immunohistochemical colocalization with brevican in perineuronal nets. *Molecular and Cellular Neurosciences*, *24*, 148–159. https://doi.org/10.1016/S1044-7431(03)00133-7

Berglöf, E., Plantman, S., Johansson, S., & Strömberg, I. (2008). Inhibition of proteoglycan synthesis affects neuronal outgrowth and astrocytic migration in organotypic cultures of fetal ventral mesencephalon. *Journal of Neuroscience Research*, *86*, 84–92. https://doi.org/10.1002/jnr.21465

Bertolino, A., Rubino, V., Sambataro, F., Blasi, G., Latorre, V., Fazio, L., … Scarabino, T. (2006). Prefrontal-hippocampal coupling during memory processing is modulated by COMT val158met genotype. *Biological Psychiatry*, *60*, 1250–1258. https://doi.org/10.1016/j.biopsych.2006.03.078

Bogerts, B., Ashtari, M., Degreef, G., Alvir, J. M., Bilder, R. M., & Lieberman, J. A. (1990). Reduced temporal limbic structure volumes on magnetic resonance images in first episode schizophrenia. *Psychiatry Research*, *35*, 1–13. https://doi.org/10.1016/0925-4927(90)90004-P

Bogerts, B., Lieberman, J. A., Ashtari, M., Bilder, R. M., Degreef, G., Lerner, G., … Masiar, S. (1993). Hippocampus-amygdala volumes and psychopathology in chronic schizophrenia. *Biological Psychiatry*, *33*, 236–246. https://doi.org/10.1016/0006-3223(93)90289-P

Buckley, P. F. (2019). Neuroinflammation and Schizophrenia. *Current Psychiatry Reports*, *21*, 72. https://doi.org/10.1007/s11920-019-1050-z

Button, K. S., Ioannidis, J. P., Mokrysz, C., Nosek, B. A., Flint, J., Robinson, E. S., & Munafò, M. R. (2013). Power failure: Why small sample size undermines the reliability of neuroscience. *Nature Reviews Neuroscience*, *14*, 365–376. https://doi.org/10.1038/nrn3475

Chelini, G., Pantazopoulos, H., Durning, P., & Berretta, S. (2018). The tetrapartite synapse: A key concept in the pathophysiology of schizophrenia. *European Psychiatry: The Journal of the Association*

of European Psychiatrists, *50*, 60–69. https://doi.org/10.1016/j.eurpsy.2018.02.003

Chepenik, L. G., Wang, F., Spencer, L., Spann, M., Kalmar, J. H., Womer, F., … Blumberg, H. P. (2012). Structure-function associations in hippocampus in bipolar disorder. *Biological Psychology*, *90*, 18–22. https://doi.org/10.1016/j.biopsycho.2012.01.008

Christodoulou, T., Messinis, L., Papathanasopoulos, P., & Frangou, S. (2012). The impact of familial risk for schizophrenia or bipolar disorder on cognitive control during episodic memory retrieval. *Psychiatry Research*, *197*, 212–216. https://doi.org/10.1016/j.psychres.2011.12.028

Cicanic, M., Edamatsu, M., Bekku, Y., Vorisek, I., Oohashi, T., & Vargova, L. (2018). A deficiency of the link protein Bral2 affects the size of the extracellular space in the thalamus of aged mice. *Journal of Neuroscience Research*, *96*, 313–327. https://doi.org/10.1002/jnr.24136

Cichon, S., Muhleisen, T. W., Degenhardt, F. A., Mattheisen, M., Miro, X., Strohmaier, J., … Nothen, M. M. (2011). Genome-wide association study identifies genetic variation in neurocan as a susceptibility factor for bipolar disorder. *American Journal of Human Genetics*, *88*, 372–381. https://doi.org/10.1016/j.ajhg.2011.01.017

Crowley, S. J., Tanner, J. J., Ramon, D., Schwab, N. A., Hizel, L. P., & Price, C. C. (2018). Reliability and utility of manual and automated estimates of total intracranial volume. *Journal of the International Neuropsychological Society: JINS*, *24*, 206–211. https://doi.org/10.1017/S1355617717000868

Dannlowski, U., Kugel, H., Grotegerd, D., Redlich, R., Suchy, J., Opel, N., … Witt, S. H. (2015). NCAN cross-disorder risk variant is associated with limbic gray matter deficits in healthy subjects and major depression. *Neuropsychopharmacology: Official Publication of the American College of Neuropsychopharmacology*, *40*, 2510–2516. https://doi.org/10.1038/npp.2015.86

Düzel, E., Berron, D., Schütze, H., Cardenas-Blanco, A., Metzger, C., Betts, M., … Jessen, F. (2018). CSF total tau levels are associated with hippocampal novelty irrespective of hippocampal volume. *Alzheimer's & Dementia (Amsterdam, Netherlands)*, *10*, 782–790. https://doi.org/10.1016/j.dadm.2018.10.003

Düzel, E., Schütze, H., Yonelinas, A. P., & Heinze, H.-J. (2011). Functional phenotyping of successful aging in long-term memory: Preserved performance in the absence of neural compensation. *Hippocampus*, *21*, 803–814.

Eickhoff, S. B., Stephan, K. E., Mohlberg, H., Grefkes, C., Fink, G. R., Amunts, K., & Zilles, K. (2005). A new SPM toolbox for combining probabilistic cytoarchitectonic maps and functional imaging data. *NeuroImage*, *25*, 1325–1335. https://doi.org/10.1016/j.neuroimage.2004.12.034

Einarsdottir, E., Peyrard-Janvid, M., Darki, F., Tuulari, J. J., Merisaari, H., Karlsson, L., … Kere, J. (2017). Identification of NCAN as a candidate gene for developmental dyslexia. *Scientific Reports*, *7*, 9294. https://doi.org/10.1038/s41598-017-10175-7

Eklund, A., Nichols, T. E., & Knutsson, H. (2016). Cluster failure: Why fMRI inferences for spatial extent have inflated false-positive rates. *Proceedings of the National Academy of Sciences of the United States of America*, *113*, 7900–7905. https://doi.org/10.1073/pnas.1602413113

Ekman, C. J., Petrovic, P., Johansson, A. G. M., Sellgren, C., Ingvar, M., & Landén, M. (2017). A history of psychosis in bipolar disorder is associated with gray matter volume reduction. *Schizophrenia Bulletin*, *43*, 99–107. https://doi.org/10.1093/schbul/sbw080

Erk, S., Meyer-Lindenberg, A., Linden, D. E. J., Lancaster, T., Mohnke, S., Grimm, O., … Walter, H. (2014). Replication of brain function effects of a genome-wide supported psychiatric risk variant in the CACNA1C gene and new multi-locus effects. *NeuroImage*, *94*, 147–154. https://doi.org/10.1016/j.neuroimage.2014.03.007

Erk, S., Meyer-Lindenberg, A., Schmierer, P., Mohnke, S., Grimm, O., Garbusow, M., … Walter, H. (2014). Hippocampal and frontolimbic function as intermediate phenotype for psychosis: Evidence from healthy relatives and a common risk variant in CACNA1C. *Biological Psychiatry*, *76*, 466–475. https://doi.org/10.1016/j.biopsych.2013.11.025

Erk, S., Meyer-Lindenberg, A., Schnell, K., Opitz von Boberfeld, C., Esslinger, C., Kirsch, P., … Walter, H. (2010). Brain function in carriers of a genome-wide supported bipolar disorder variant. *Archives of General Psychiatry*, *67*, 803–811. https://doi.org/10.1001/archgenpsychiatry.2010.94

Faul, F., Erdfelder, E., Buchner, A., & Lang, A.-G. (2009). Statistical power analyses using G*Power 3.1: Tests for correlation and regression analyses. *Behavior Research Methods*, *41*, 1149–1160. https://doi.org/10.3758/BRM.41.4.1149

Faul, F., Erdfelder, E., Lang, A.-G., & Buchner, A. (2007). G*Power 3: A flexible statistical power analysis program for the social, behavioral, and biomedical sciences. *Behavior Research Methods*, *39*, 175–191. https://doi.org/10.3758/BF03193146

Fera, F., Passamonti, L., Cerasa, A., Gioia, M. C., Liguori, M., Manna, I., … Quattrone, A. (2013). The BDNF Val66Met polymorphism has opposite effects on memory circuits of multiple sclerosis patients and controls. *PLoS One*, *8*, e61063. https://doi.org/10.1371/journal.pone.0061063

Francis, A. N., Seidman, L. J., Tandon, N., Shenton, M. E., Thermenos, H. W., Mesholam-Gately, R. I., … Keshavan, M. S. (2013). Reduced subicular subdivisions of the hippocampal formation and verbal declarative memory impairments in young relatives at risk for schizophrenia. *Schizophrenia Research*, *151*, 154–157. https://doi.org/10.1016/j.schres.2013.10.002

Fransen, N. L., Crusius, J. B. A., Smolders, J., Mizee, M. R., van Eden, C. G., Luchetti, S., … Huitinga, I. (2020). Post-mortem multiple sclerosis lesion pathology is influenced by single nucleotide polymorphisms. *Brain Pathology (Zurich, Switzerland)*, *30*, 106–119. https://doi.org/10.1111/bpa.12760

Friston, K. J., Liddle, P. F., Frith, C. D., Hirsch, S. R., & Frackowiak, R. S. (1992). The left medial temporal region and schizophrenia. A PET study. *Brain: A Journal of Neurology*, *115* (Pt 2), 367–382.

Gogolla, N., Galimberti, I., Deguchi, Y., & Caroni, P. (2009). Wnt signaling mediates experience-related regulation of synapse numbers and mossy fiber connectivities in the adult hippocampus. *Neuron*, *62*, 510–525. https://doi.org/10.1016/j.neuron.2009.04.022

Gvozdanovic G., Stämpfli P., Seifritz E., & Rasch B. (2020). Structural brain differences predict early traumatic memory processing. *Psychophysiology*, *57*, (1). https://doi.org/10.1111/psyp.13354

Happel, M. F. K., Niekisch, H., Castiblanco Rivera, L. L., Ohl, F. W., Deliano, M., & Frischknecht, R. (2014). Enhanced cognitive flexibility in reversal learning induced by removal of the extracellular matrix in auditory cortex. *Proceedings of the National Academy of Sciences of the United States of America*, *111*, 2800–2805. https://doi.org/10.1073/pnas.1310272111

Helmstaedter, C., Lendt, M., & Lux, S. (2001). *Verbaler Lern- und Merkfähigkeitstest. VLMT; Manual*. Göttingen: Beltz-Test.

Hinrichs H., Scholz M., Tempelmann C., Woldorff M. G., Dale A. M., & Heinze H. -J. (2000). Deconvolution of Event-Related fMRI Responses in Fast-Rate Experimental Designs: Tracking Amplitude Variations. *Journal of Cognitive Neuroscience*, *12*, (supplement 2), 76–89. https://doi.org/10.1162/089892900564082

Ioannidis, J. P. (2008). Why most discovered true associations are inflated. *Epidemiology*, *19*, 640–648. https://doi.org/10.1097/EDE.0b013e31818131e7

Jessen, F., Spottke, A., Boecker, H., Brosseron, F., Buerger, K., Catak, C., … Düzel, E. (2018). Design and first baseline data of the DZNE multicenter observational study on predementia Alzheimer's disease (DELCODE). *Alzheimer's Research & Therapy*, *10*, 15. https://doi.org/10.1186/s13195-017-0314-2

Kauppi, K., Nilsson, L. G., Adolfsson, R., Eriksson, E., & Nyberg, L. (2011). KIBRA polymorphism is related to enhanced memory and elevated hippocampal processing. *Journal of Neuroscience*, *31*, 14218–14222. https://doi.org/10.1523/JNEUROSCI.3292-11.2011

Krach, S., Jansen, A., Krug, A., Markov, V., Thimm, M., Sheldrick, A. J., … Kircher, T. (2010). COMT genotype and its role on hippocampal-prefrontal regions in declarative memory. *NeuroImage*, *53*, 978–984. https://doi.org/10.1016/j.neuroimage.2009.12.090

Krämer, U. M., Cunillera, T., Càmara, E., Marco-Pallarés, J., Cucurell, D., Nager, W., … Münte, T. F. (2007). The impact of catechol-O-methyltransferase and dopamine D4 receptor genotypes on neurophysiological markers of performance monitoring. *Journal of Neuroscience*, *27*, 14190–141908. https://doi.org/10.1523/JNEUROSCI.4229-07.2007

Lieberman, J. A., Girgis, R. R., Brucato, G., Moore, H., Provenzano, F., Kegeles, L., … Small, S. A. (2018). Hippocampal dysfunction in the pathophysiology of schizophrenia: A selective review and hypothesis for early detection and intervention. *Molecular Psychiatry*, *23*, 1764–1772. https://doi.org/10.1038/mp.2017.249

Lisman, J. E., Coyle, J. T., Green, R. W., Javitt, D. C., Benes, F. M., Heckers, S., & Grace, A. A. (2008). Circuit-based framework for understanding neurotransmitter and risk gene interactions in schizophrenia. *Trends in Neurosciences*, *31*, 234–242. https://doi.org/10.1016/j.tins.2008.02.005

Lisman, J. E., & Grace, A. A. (2005). The hippocampal-VTA loop: Controlling the entry of information into long-term memory. *Neuron*, *46*, 703–713. https://doi.org/10.1016/j.neuron.2005.05.002

Lodge, D. J., & Grace, A. A. (2007). Aberrant hippocampal activity underlies the dopamine dysregulation in an animal model of schizophrenia. *The Journal of Neuroscience: The Official Journal of the Society for Neuroscience*, *27*, 11424–11430. https://doi.org/10.1523/JNEUROSCI.2847-07.2007

Meyer-Puttlitz, B., Milev, P., Junker, E., Zimmer, I., Margolis, R. U., & Margolis, R. K. (1995). Chondroitin sulfate and chondroitin/keratan sulfate proteoglycans of nervous tissue: Developmental changes of neurocan and phosphacan. *Journal of Neurochemistry*, *65*, 2327–2337. https://doi.org/10.1046/j.1471-4159.1995.65052327.x

Miró, X., Meier, S., Dreisow, M. L., Frank, J., Strohmaier, J., Breuer, R., … Zimmer, A. (2012). Studies in humans and mice implicate neurocan in the etiology of mania. *The American Journal of Psychiatry*, *169*, 982–990. https://doi.org/10.1176/appi.ajp.2012.11101585

Mitlöhner, J., Kaushik, R., Niekisch, H., Blondiaux, A., Gee, C. E., Happel, M. F. K., … Seidenbecher, C. (2020). Dopamine receptor activation modulates the integrity of the perisynaptic extracellular matrix at excitatory synapses. *Cells*, *9*(2), 260. https://doi.org/10.3390/cells9020260

Mühleisen, T. W., Mattheisen, M., Strohmaier, J., Degenhardt, F., Priebe, L., Schultz, C. C., … Cichon, S. (2012). Association between schizophrenia and common variation in neurocan (NCAN), a genetic risk factor for bipolar disorder. *Schizophrenia Research*, *138*, 69–73. https://doi.org/10.1016/j.schres.2012.03.007

Nenadic, I., Maitra, R., Langbein, K., Dietzek, M., Lorenz, C., Smesny, S., … Gaser, C. (2015). Brain structure in schizophrenia vs. psychotic bipolar I disorder: A VBM study. *Schizophrenia Research*, *165*, 212–219. https://doi.org/10.1016/j.schres.2015.04.007

Oertel-Knöchel, V., Reinke, B., Feddern, R., Knake, A., Knöchel, C., Prvulovic, D., … Linden, D. E. J. (2014). Episodic memory impairments in bipolar disorder are associated with functional and structural brain changes. *Bipolar Disorders*, *16*, 830–845. https://doi.org/10.1111/bdi.12241

Palaniyappan, L., Balain, V., & Liddle, P. F. (2012). The neuroanatomy of psychotic diathesis: A meta-analytic review. *Journal of Psychiatric Research*, *46*, 1249–1256. https://doi.org/10.1016/j.jpsychires.2012.06.007

Pantazopoulos, H., & Berretta, S. (2016). In sickness and in health: Perineuronal nets and synaptic plasticity in psychiatric disorders. *Neural Plasticity*, *2016*, 9847696. https://doi.org/10.1155/2016/9847696

Piras, F., Schiff, M., Chiapponi, C., Bossu, P., Muhlenhoff, M., Caltagirone, C., … Spalletta, G. (2015). Brain structure, cognition and negative symptoms in schizophrenia are associated with serum levels of polysialic acid-modified NCAM. *Translational Psychiatry*, *5*, e658. https://doi.org/10.1038/tp.2015.156

Preston, A. R., Shohamy, D., Tamminga, C. A., & Wagner, A. D. (2005). Hippocampal function, declarative memory, and schizophrenia: Anatomic and functional neuroimaging considerations. *Current Neurology and Neuroscience Reports*, *5*, 249–256. https://doi.org/10.1007/s11910-005-0067-3

Psychiatric GWAS Bipolar Disorder Working Group (2011). Large-scale genome-wide association analysis of bipolar disorder identifies a new susceptibility locus near ODZ4. *Nature Genetics*, *43*, 977–983.

Ragland, J. D., Laird, A. R., Ranganath, C., Blumenfeld, R. S., Gonzales, S. M., & Glahn, D. C. (2009). Prefrontal activation deficits during episodic memory in schizophrenia. *The American Journal of Psychiatry*, *166*, 863–874. https://doi.org/10.1176/appi.ajp.2009.08091307

Rauch, U., Feng, K., & Zhou, X. H. (2001). Neurocan: A brain chondroitin sulfate proteoglycan. *Cellular and Molecular Life Sciences: CMLS*, *58*, 1842–1856.

Raum, H., Dietsche, B., Nagels, A., Witt, S. H., Rietschel, M., Kircher, T., & Krug, A. (2015). A genome-wide supported psychiatric risk variant in NCAN influences brain function and cognitive performance in healthy subjects. *Human Brain Mapping*, *36*, 378–390.

Richter, A., Barman, A., Wüstenberg, T., Soch, J., Schanze, D., Deibele, A., … Schott, B. H. (2017). Behavioral and neural manifestations of reward memory in carriers of low-expressing versus high-expressing genetic variants of the dopamine D2 receptor. *Frontiers in Psychology*, *8*, 654. https://doi.org/10.3389/fpsyg.2017.00654

Richter, S., Gorny, X., Marco-Pallares, J., Krämer, U. M., Machts, J., Barman, A., … Schott, B. H. (2011). A potential role for a genetic variation of AKAP5 in human aggression and anger control. *Frontiers in Human Neuroscience*, *5*, 175. https://doi.org/10.3389/fnhum.2011.00175

Rimol, L. M., Hartberg, C. B., Nesvåg, R., Fennema-Notestine, C., Hagler, D. J., Pung, C. J., … Agartz, I. (2010). Cortical thickness

and subcortical volumes in schizophrenia and bipolar disorder. *Biological Psychiatry*, *68*, 41–50. https://doi.org/10.1016/j.biopsych.2010.03.036

Saleem, S., Kumar, D., & Venkatasubramanian, G. (2018). Prospective memory in first-degree relatives of patients with schizophrenia. *The Clinical Neuropsychologist*, *32*, 993–1001. https://doi.org/10.1080/13854046.2017.1406145

Schizophrenia Psychiatric genomics GWAS consortium (2011). Genome-wide association study identifies five new schizophrenia loci. *Nature Genetics*, *43*, 969–976.

Schobel, S. A., Lewandowski, N. M., Corcoran, C. M., Moore, H., Brown, T., Malaspina, D., & Small, S. A. (2009). Differential targeting of the CA1 subfield of the hippocampal formation by schizophrenia and related psychotic disorders. *Archives of General Psychiatry*, *66*, 938–946. https://doi.org/10.1001/archgenpsychiatry.2009.115

Schott, B. H., Assmann, A., Schmierer, P., Soch, J., Erk, S., Garbusow, M., … Walter, H. (2014). Epistatic interaction of genetic depression risk variants in the human subgenual cingulate cortex during memory encoding. *Translational Psychiatry*, *4*, e372. https://doi.org/10.1038/tp.2014.10

Schott, B. H., Seidenbecher, C. I., Fenker, D. B., Lauer, C. J., Bunzeck, N., Bernstein, H. G., … Düzel, E. (2006). The dopaminergic midbrain participates in human episodic memory formation: Evidence from genetic imaging. *Journal of Neuroscience*, *26*, 1407–1417. https://doi.org/10.1523/JNEUROSCI.3463-05.2006

Schott, B. H., Voss, M., Wagner, B., Wüstenberg, T., Düzel, E., & Behr, J. (2015). Fronto-limbic novelty processing in acute psychosis: Disrupted relationship with memory performance and potential implications for delusions. *Frontiers in Behavioral Neuroscience*, *9*, 144. https://doi.org/10.3389/fnbeh.2015.00144

Schubert C. R., O'Donnell P., Quan J., Wendland J. R., Xi H. S., Winslow A. R., … Weinberger D. R. (2015). BrainSeq: Neurogenomics to drive novel target discovery for neuropsychiatric disorders. *Neuron*, *88*, (6), 1078–1083. https://doi.org/10.1016/j.neuron.2015.10.047

Schultz, C. C., Muhleisen, T. W., Nenadic, I., Koch, K., Wagner, G., Schachtzabel, C., … Schlosser, R. G. M. (2014). Common variation in NCAN, a risk factor for bipolar disorder and schizophrenia, influences local cortical folding in schizophrenia. *Psychological Medicine*, *44*, 811–820.

Schulze, T. G., Akula, N., Breuer, R., Steele, J., Nalls, M. A., Singleton, A. B., … McMahon, F. J. (2014). Molecular genetic overlap in bipolar disorder, schizophrenia, and major depressive disorder. *The World Journal of Biological Psychiatry: The Official Journal of the World Federation of Societies of Biological Psychiatry*, *15*, 200–208. https://doi.org/10.3109/15622975.2012.662282

Schwarzkopf, D. S., de Haas, B., & Rees, G. (2012). Better ways to improve standards in brain-behavior correlation analysis. *Frontiers in Human Neuroscience*, *6*, 200. https://doi.org/10.3389/fnhum.2012.00200

Sim, H., Hu, B., & Viapiano, M. S. (2009). Reduced expression of the hyaluronan and proteoglycan link proteins in malignant gliomas. *The Journal of Biological Chemistry*, *284*, 26547–26556. https://doi.org/10.1074/jbc.M109.013185

Skelley, S. L., Goldberg, T. E., Egan, M. F., Weinberger, D. R., & Gold, J. M. (2008). Verbal and visual memory: Characterizing the clinical and intermediate phenotype in schizophrenia. *Schizophrenia Research*, *105*, 78–85. https://doi.org/10.1016/j.schres.2008.05.027

Smeland, O. B., Bahrami, S., Frei, O., Shadrin, A., O'Connell, K., Savage, J., … Andreassen, O. A. (2019). Genome-wide analysis reveals extensive genetic overlap between schizophrenia, bipolar disorder, and intelligence. *Molecular Psychiatry*, *25*(4), 844–853. https://doi.org/10.1038/s41380-018-0332-x

Spicer, A. P., Joo, A., & Bowling, R. A. (2003). A hyaluronan binding link protein gene family whose members are physically linked adjacent to chondroitin sulfate proteoglycan core protein genes: The missing links. *The Journal of Biological Chemistry*, *278*, 21083–21091.

Squire, L. R., Stark, C. E. L., & Clark, R. E. (2004). The medial temporal lobe. *Annual Review of Neuroscience*, *27*, 279–306. https://doi.org/10.1146/annurev.neuro.27.070203.144130

Suazo, V., Díez, Á., Tamayo, P., Montes, C., & Molina, V. (2013). Limbic hyperactivity associated to verbal memory deficit in schizophrenia. *Journal of Psychiatric Research*, *47*, 843–850. https://doi.org/10.1016/j.jpsychires.2013.02.007

Sucha, P., Chmelova, M., Kamenicka, M., Bochin, M., Oohashi, T., & Vargova, L. (2020). The effect of Hapln4 link protein deficiency on extracellular space diffusion parameters and perineuronal nets in the auditory system during aging. *Neurochemical Research*, *45*, 68–82. https://doi.org/10.1007/s11064-019-02894-2

Talati, P., Rane, S., Kose, S., Blackford, J. U., Gore, J., Donahue, M. J., & Heckers, S. (2014). Increased hippocampal CA1 cerebral blood volume in schizophrenia. *NeuroImage. Clinical*, *5*, 359–364.

Tregellas, J. R., Smucny, J., Harris, J. G., Olincy, A., Maharajh, K., Kronberg, E., … Freedman, R. (2014). Intrinsic hippocampal activity as a biomarker for cognition and symptoms in schizophrenia. *The American Journal of Psychiatry*, *171*, 549–556. https://doi.org/10.1176/appi.ajp.2013.13070981

Vita, A., de Peri, L., Silenzi, C., & Dieci, M. (2006). Brain morphology in first-episode schizophrenia: A meta-analysis of quantitative magnetic resonance imaging studies. *Schizophrenia Research*, *82*, 75–88. https://doi.org/10.1016/j.schres.2005.11.004

Wang, L., Liu, W., Li, X., Xiao, X., Li, L., Liu, F., … Li, M. (2018). Further evidence of an association between NCAN rs1064395 and bipolar disorder. *Molecular Neuropsychiatry*, *4*, 30–34.

Wang, P., Cai, J., Ni, J., Zhang, J., Tang, W., & Zhang, C. (2016). The NCAN gene: Schizophrenia susceptibility and cognitive dysfunction. *Neuropsychiatric Disease and Treatment*, *12*, 2875–2883.

Wegman, J., Tyborowska, A., Hoogman, M., Arias Vásquez, A., & Janzen, G. (2017). The brain-derived neurotrophic factor Val66Met polymorphism affects encoding of object locations during active navigation. *The European Journal of Neuroscience*, *45*, 1501–1511. https://doi.org/10.1111/ejn.13416

Weise, C. M., Bachmann, T., Schroeter, M. L., & Saur, D. (2019). When less is more: Structural correlates of core executive functions in young adults – A VBM and cortical thickness study. *NeuroImage*, *189*, 896–903. https://doi.org/10.1016/j.neuroimage.2019.01.070

Yarkoni, T. (2009). Big Correlations in Little Studies: Inflated fMRI Correlations Reflect Low Statistical Power—Commentary on Vul et al. (2009). *Perspectives on Psychological Science*, *4*, (3), 294–298. https://doi.org/10.1111/j.1745-6924.2009.01127.x

Zhou, X. H., Brakebusch, C., Matthies, H., Oohashi, T., Hirsch, E., Moser, M., … Fassler, R. (2001). Neurocan is dispensable for brain development. *Molecular and Cellular Biology*, *21*, 5970–5978. https://doi.org/10.1128/MCB.21.17.5970-5978.2001

Zierhut, K., Bogerts, B., Schott, B., Fenker, D., Walter, M., Albrecht, D., … Schiltz, K. (2010). The role of hippocampus dysfunction in

deficient memory encoding and positive symptoms in schizophrenia. *Psychiatry Research*, *183*, 187–194. https://doi.org/10.1016/j.pscychresns.2010.03.007

SUPPORTING INFORMATION

Additional supporting information may be found online in the Supporting Information section.

How to cite this article: Assmann A, Richter A, Schütze H, et al. Neurocan genome-wide psychiatric risk variant affects explicit memory performance and hippocampal function in healthy humans. *Eur J Neurosci*. 2020;00:1–18. https://doi.org/10.1111/ejn.14872